Akihiko Kondo ORCID iD: 0000-0003-1527-5288

Jun Ishii ORCID iD: 0000-0003-2568-515X

Yasuyuki Nakamura ORCID iD: 0000-0002-0093-3754

Kenta Morita ORCID iD: 0000-0002-2156-4812

Tatsuo Maruyama ORCID iD: 0000-0003-2428-1911

Manuscript Type: Articles

Comparative analyses of site-directed mutagenesis of human melatonin MTNR1A and MTNR1B receptors using a yeast fluorescent biosensor

Yasuyuki Nakamura,[1,2] Ririka Asama,[2] Takuya Tabata,[2] Kenta Morita,[3] Tatsuo Maruyama,[3] Akihiko Kondo,[1,2,3] Jun Ishii[1,2,*]

[1] Engineering Biology Research Center, Kobe University, Kobe, Japan

[2] Graduate School of Science, Technology and Innovation, Kobe University, Kobe, Japan

This article has been accepted for publication and undergone full peer review but has not been through the copyediting, typesetting, pagination and proofreading process, which may lead to differences between this version and the Version of Record. Please cite this article as doi: 10.1002/bit.27609.

[3] Department of Chemical Science and Engineering, Graduate School of Engineering, Kobe University, Kobe, Japan

***Corresponding author:** Jun Ishii

Engineering Biology Research Center, Kobe University, 1-1 Rokkodai, Nada, Kobe 657-8501, Japan

Tel: +81-78-803-6356; Fax: +81-78-803-6192; E-mail: junjun@port.kobe-u.ac.jp

Abstract

Melatonin is an indoleamine neurohormone made by the pineal gland. Its receptors, MTNR1A and MTNR1B, are members of the G-protein-coupled receptor (GPCR) family and are involved in sleep, circadian rhythm and mood disorders, and in the inhibition of cancer growth. These receptors therefore represent significant molecular targets for insomnia, circadian sleep disorders, and cancer. The yeast *Saccharomyces cerevisiae* is an attractive host for assaying agonistic activity for human GPCR. We previously constructed a GPCR-based biosensor employing a high-sensitivity yeast strain that incorporated both a chimeric yeast-human Gα protein and a bright

fluorescent reporter gene (*ZsGreen*). Similar approaches have been used for simple and convenient measurements of various GPCR activities. In the current study, we constructed a fluorescence-based yeast biosensor for monitoring the signaling activation of human melatonin receptors. We used this system to analyze point mutations, including previously unreported mutations of the consensus sequences of MTNR1A and MTNR1B melatonin receptors, and compared their effects. Most mutations in the consensus sequences significantly affected the signaling capacities of both receptors, but several mutations showed differences between these subtype receptors. Thus, this yeast biosensor holds promise for revealing the functions of melatonin receptors.

Graphical Abstract

A *Saccharomyces cerevisiae* fluorescence-based biosensor to detect signaling by human melatonin receptors (MTNR1A and MTNR1B) in response to melatonin was constructed in this study, which incorporates a bright fluorescent reporter (ZsGreen) and a chimeric yeast-human Gα protein, and provides higher dynamic range and high sensitivity compared to other biosensors. Nakamura and coworkers demonstrated the utility of GPCR-based biosensor for analyzing site-directed mutants of human melatonin receptors. The constructed yeast biosensor holds promise for revealing the functions of melatonin receptors.

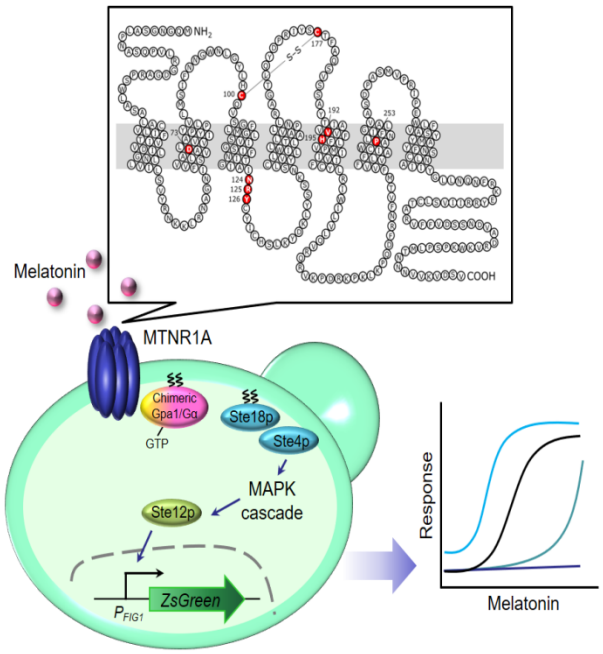

Keywords: G-protein-coupled receptor; melatonin receptor; G-protein signaling; *Saccharomyces cerevisiae*; site-directed mutagenesis

1. Introduction

Melatonin (5-methoxy-*N*-acetyltryptamine) is the major indoleamine neurohormonal product of the pineal gland, acting as a chemical signal for nighttime darkness (Reiter et al., 1991). In addition, melatonin is involved in various physiologic functions, including sleep induction, circadian rhythm regulation, and immune response (Dubocovich et al., 2010; Simonneaux and Ribelayga, 2003; Zawilska et al., 2009). Melatonin mediates its effect through two high-affinity

receptors, MTNR1A and MTNR1B (Reppert et al., 1994 and 1995). MTNR1A is a 350 amino acid protein and has 60% sequence homology with the 362 amino acid MTNR1B protein (Reppert et al., 1995). Both receptors belong to the family of seven transmembrane G-protein-coupled receptors (GPCRs) that collectively have extraordinary therapeutic potential as drug targets for a wide spectrum of diseases (Rosenbaum et al., 2007).

Melatonin receptors (MTNRs) are implicated in many biological processes, ranging from anti-inflammatory to antioxidant effects, and may be involved in Parkinson's disease (Adi et al., 2010; Delagrange et al., 2003; Ge et al., 2019; Zlotos et al., 2014). A growing body of evidence shows additional roles for melatonin in antitumor and neuroprotectant processes (Abreu et al., 2015; Blask et al., 1999; Martinez-Campa et al., 2009; Miller et al., 2015; Pandi-Perumal et al., 2006 and 2008; Vriend et al., 2015). Melatonin signaling pathways may also be involved in events leading to the development of type-2 diabetes (Lyssenko et al., 2009). It was previously reported that rare variants of the MTNR1B gene increase the risk of developing type-2 diabetes (Bonnefond et al., 2012) and thus analyzing the functions

of mutant proteins involved in type-2 diabetes could help reveal the mechanism underlying this disorder. The activation of the MTNR1A receptor is mainly implicated in the regulation of rapid eye movement (REM) sleep, whereas the MTNR1B receptor selectively increase non-REM (NREM) sleep (Gobbi and Comai, 2019). The MTNR1A receptor is located in the locus coeruleus and lateral hypothalamus (REM areas), while the MTNR1B receptor is uniquely located in the reticular thalamus, an area involved in NREM triggering (Gobbi and Comai, 2019). The development of a simple and convenient detection system for assaying MTNR activity would therefore have great potential for revealing the functions of melatonin receptors.

The eukaryotic unicellular budding yeast *Saccharomyces cerevisiae* is a useful microbial host in the synthesis of GPCR biosensors (Hashi et al., 2018; Liu et al., 2016; Minic et al., 2005). The yeast pheromone signaling pathway is non-competitive and monopolistic, and yeast serve as simplified experimental systems compared to the complicated signaling pathways used by other higher eukaryotes (Ishii et al., 2010). Many heterologous GPCRs have been functionally expressed in yeast, either through

the endogenous yeast Gα-subunit (Gpa1p) or via a yeast-human chimeric G-protein (Brown et al., 2000; Ishii et al., 2014). Yeast cells have been adapted (by the addition of enzymatic and growth reporter genes) for use in various applications, including ligand screening and receptor mutagenesis (Klco et al., 2006; Minic et al., 2005; Nakamura et al., 2013a; Scarselli et al., 2007).

A previously established fluorescent reporter gene assay for GPCRs provides a simple procedure for measuring receptor activity. The yeast cell culture is simply diluted with buffer and the fluorescence intensity is read using a flow cytometer that can be used for comparative analyses, quantitative screening, and cell sorting (Ishii et al., 2006, 2008, 2012). However, systems using enhanced green fluorescent protein (*EGFP*; derived from *Aequorea victoria*) as a reporter gene exhibit comparatively weak fluorescence (Nakamura et al., 2013a), restricting the use of *EGFP* as a reporter for various GPCRs and applications because the low signal-to-noise (S/N) ratio limits detection. We previously developed a refined GPCR-based fluorescence biosensor by using the tetrameric *Zoanthus* sp. green fluorescent protein (encoded by *ZsGreen*) and showed that ZsGreen emits brighter fluorescence than EGFP when used as a reporter

in yeast (Nakamura et al., 2013a). Specifically, a previously described EGFP reporter yeast strain was re-engineered by replacing a pair of *EGFP* reporter genes with *ZsGreen* genes, and replacing the endogenous *GPA1* locus with a chimeric gene coding for a yeast Gpa1-human $G\alpha_{i3}$ protein (Gpa1/$G\alpha_{i3}$ transplant; G_{i3}tp). The re-engineered yeast strain showed over 30-fold increased fluorescence compared to the previous *EGFP* reporter strain. This improved system was used to detect agonist-promoted signaling by several human GPCRs whose natural ligands are short peptides, such as neurotensin, somatostatin, and angiotensin (Hashi et al., 2018; Nakamura et al., 2013a, 2014), and a monoamine serotonin (Nakamura et al., 2015).

In the present study, we constructed a fluorescence-based microbial yeast biosensor that can monitor the activation of human melatonin receptor signaling in response to melatonin. Living yeast cells harboring *ZsGreen* reporter genes and a *G_{i3}tp* gene were used to analyze MTNR1A and MTNR1B signaling. *ZsGreen*-inducing MTNR-expressing strains exhibited much higher levels of fluorescence than *EGFP*-inducing MTNR-expressing yeast strains and showed a higher dynamic range for melatonin stimulation. We additionally demonstrated that

our yeast biosensor strain allows the analysis of point mutations on the MTNR1A and MTNR1B receptors to compare the mutations in consensus sequences of the two receptors. We evaluated the signal functions of several mutated melatonin receptors, including mutants not previously reported. Several mutations significantly affected the signaling capacity of melatonin receptors and increased their basal signaling activity. This increase of basal (constitutive) signaling activity was not observed in the previous yeast system, suggesting that our re-engineered yeast fluorescent GPCR biosensor has high sensitivity. Thus, this yeast biosensor holds promise for revealing the functions of melatonin receptors.

2. Materials and Methods

2.1. Plasmid Construction

All plasmids used in this study are listed in Table 1. All primers used for plasmid construction are listed in Supporting Information Table S1.

DNA fragments encoding the human MTNR1A and MTNR1B proteins (human original sequences without codon optimizations) were PCR-amplified from

pPR3-MTNR1A and pPR3-MTNR1B (Nakamura et al., 2013b) using primers #1 and #2 (for MTNR1A) and #3 and #4 (for MTNR1B). The resulting amplicons were digested with *Nhe*I+*Sal*I, then ligated between the *PGK1* promoter (P_{PGK1}) and the *PGK1* terminator (T_{PGK1}) in similarly digested pGK421 (Togawa et al., 2010) to yield the plasmids pGK421-MTNR1A and pGK421-MTNR1B, respectively.

The plasmids for expressing mutated MTNR1A proteins were constructed as follows. To introduce site-directed mutations, gene fragments encoding the upstream and downstream parts of mutated MTNR1A were respectively PCR-amplified from pGK421-MTNR1A using primer pairs #1 + #5, #7, #9, #11, #13, #15, #17, #19, #21 or #23, and #6, #8, #10, #12, #14, #16, #18, #20, #22 or #24 + #2 (for D73N, C100A, N124A, R125A, Y126A, C177A, V192T, H195A, V192T+H195A or P253A, respectively). These amplified fragments were then used as templates for overlap PCR with primers #1 and #2. The resulting mutated *MTNR1A* amplicons were digested with *Nhe*I+*Sal*I and ligated into similarly digested pGK421, resulting in the plasmids designated pGK421-MTNR1A-D73N, -C100A, -N124A, -R125A, -Y126A, -C177A, -V192T, -H195A, -V192T+H195A or -P253A, respectively.

The plasmids for expressing mutated MTNR1B proteins were constructed as follows. To introduce point mutations, gene fragments encoding the upstream and downstream parts of mutated MTNR1B were respectively PCR-amplified from pGK421-MTNR1B using primer pairs #3 + #25, #27, #29, #31, #33, #35, #37, #39, #41 or #43, and #26, #28, #30, #32, #34, #36, #38, #40, #42 or #44 + #4 (for D86N, C113A, N137A, R138A, Y139A, C190A, V205T, H208A, V205T+H208A or P266A, respectively). These amplified fragments were then used as templates for overlap PCR with primers #3 and #4. The resulting mutated *MTNR1B* amplicons were digested with *Nhe*I+*Sal*I and ligated into similarly digested pGK421, resulting in the plasmids designated pGK421-MTNR1B-D86N, -C113A, -N137A, -R138A, -Y139A, -C190A, -V205T, -H208A, -V205T+H208A or -P266A, respectively.

The plasmids for expressing the mutated MTNR1A and MTNR1B fusion proteins C-terminally linked to the monomeric mUkG fluorescent protein were constructed as follows. DNA fragments containing the mutated *MTNR1A* gene (without a stop codon) were PCR-amplified from pGK421-MTNR1A-xxx (xxx: D73N, C100A, N124A, R125A, Y126A, C177A, V192T, H195A, V192T+H195A or

P253A, respectively) using primers #1 and #45. The resulting amplicons were digested with *Nhe*I+*Sal*I, then ligated between the *PGK1* promoter (P_{PGK1}) and the *mUkG1* gene in a manner similar to pGK421-NTSR1-mUkG constructed previously (Hashi et al., 2018), yielding the plasmids pGK421-MTNR1A-xxx-mUkG (xxx: D73N, C100A, N124A, R125A, Y126A, C177A, V192T, H195A, V192T+H195A or P253A, respectively). The plasmids pGK421-MTNR1B-xxx-mUkG (xxx: D86N, C113A, N137A, R138A, Y139A, C190A, V205T, H208A, V205T+H208A or P266A, respectively) were similarly constructed with primers #3 and #46.

2.2. Yeast Strains and Media

All yeast strains used in this study are listed in Table 1. Transformation with plasmids was performed using the lithium acetate method (Gietz et al., 1992).

Synthetic dextrose (SD) medium contained 6.7 g/L yeast nitrogen base without amino acids (YNB) (BD-Diagnostic Systems, Sparks, MD, USA) and 20 g/L glucose. As described previously (Ishii et al., 2014), SDM71 medium was prepared by adjusting SD medium to pH 7.1 with 200 mM 3-(*N*-morpholino)-2-hydroxypropanesulfonic acid (MOPSO) (Nacalai Tesque, Kyoto,

Japan). YPD medium contained 10 g/L yeast extract (Nacalai Tesque), 20 g/L peptone (BD-Diagnostic Systems) and 20 g/L glucose. Amino acids and nucleotides (20 mg/L histidine, 60 mg/L leucine, and 20 mg/L uracil; without methionine) were added to SD or SDM71 medium to compensate for relevant auxotrophies. For solid medium, agar was added at 20 g/L.

2.3. MTNR1A and MTNR1B Signaling Assays

The MTNR1A and MTNR1B signaling assays followed previously described procedures (Nakamura et al., 2013a, 2014, 2015) except for changes in the ligands. In brief, to assay signal activation from human MTNR1A or MTNR1B, yeast strains transformed with wild-type or mutated MTNR1A and MTNR1B expression plasmids were grown in SD medium at 30 °C overnight, then the cells were inoculated into 5 mL of the respective fresh SD medium to give an initial optical density of 0.03 at 600 nm (OD_{600} = 0.03). The cells were incubated at 30 °C on a rotary shaker at 150 rpm for up to 18 h, then harvested, washed, and resuspended in water to yield an OD_{600} = 10. The resulting yeast cell suspensions were added (at 10 μL/well; OD_{600} = 1) to the wells of 96-well cluster dishes containing fresh SDM71 medium (80 μL/well)

supplemented with 10× concentrated melatonin (Sigma-Aldrich, St. Louis, MO, USA) (10 μL/well) at various concentrations or with distilled water (without melatonin; control). The plates were incubated at 30 °C with shaking (150 rpm) for 4 h, then the samples were diluted with 1 mL of sheath fluid and fluorescence was analyzed by flow cytometry (see below).

Half maximal effective concentration (EC_{50}) values were determined using KaleidaGraph4.0 to fit the data to a dose-response logistic model.

2.4. Flow Cytometry Analysis

Flow cytometry measurements of green fluorescence followed the previously described procedure (Nakamura et al., 2015). In brief, fluorescent cells were detected using a BD FACSCanto II flow cytometer equipped with a 488-nm blue laser (Becton, Dickinson and Company, Franklin Lakes, NJ, USA) and the data were analyzed using BD FACSDiva software (v5.0; Becton, Dickinson and Company). The GFP fluorescence signal was collected through a 530/30 nm band-pass filter and the GFP-A mean of 10,000 cells was defined as ‘green fluorescence intensity’.

2.5. Measurements of the Relative Expression Levels of the mUkG-Fused MTNR1A and MTNR1B Receptors

Yeast transformants were grown in SD medium (supplemented as needed) at 30 °C overnight, then the cells were inoculated into 5 mL of the respective fresh SD medium to give an initial OD_{600} = 0.03. The cells were incubated at 30 °C on a rotary shaker at 150 rpm for up to 18 h, then the yeast cells were diluted with 1 mL of sheath fluid and fluorescence was analyzed by flow cytometry. The relative fluorescence intensity was determined as the relative level of the green fluorescence intensity of each strain expressing mUkG-fused mutated receptor against that expressing mUkG-fused wild-type MTNR1A or MTNR1B receptor.

2.6. Confocal Imaging

Yeast transformants were grown in SD medium (supplemented as needed) at 30 °C overnight, then the cells were inoculated into 5 mL of the respective fresh SD medium to give an initial OD_{600} = 0.03. The cells were incubated at 30 °C on a rotary shaker at 150 rpm for up to 18 h. Next, the cultured cells were then collected by centrifugation, and suspended in distilled water. The cell suspensions were observed

using an FV3000-IX83 confocal laser scanning microscope (CLSM; Olympus, Tokyo, Japan).

2.7. Data Analysis

Data represent the mean ± standard deviation for $n = 3$ (representing three independent transformants). The response (or maximal percentage increase: $\%E_{max}$) was expressed as the (maximal) percentage increase in the presence of melatonin at the indicated concentrations over the respective basal (unstimulated) mean fluorescence intensity value.

2.8. Modeling of the MTNR1A and MTNR1B Structures

Human MTNR1A and MTNR1B were modeled using the SWISS-MODEL server (https://swissmodel.expasy.org/) and the structure of human MTNR1A (6ME2, https://www.rcsb.org/structure/6me2) (Stauch et al., 2019) and MTNR1B (6ME6, https://www.rcsb.org/structure/6me6) (Johansson et al., 2019), respectively. Figures were created using PDBjViewer (Kinoshita and Nakamura, 2004)

3. Results and Discussion

3.1. Comparing the Agonistic Sensitivities of MTNR1A- and MTNR1B-Expressing Yeast Strains with Different Reporters and G-proteins

Our primary aim was to construct a fluorescence-based yeast biosensor with a higher dynamic range compared to conventional systems for monitoring melatonin-promoted signal transduction via human MTNR1A and MTNR1B. Our second aim was to assess the utility of the biosensor for analyzing site-directed mutant receptor proteins. In addition, since MTNR1A and MTNR1B share a high degree of sequence homology, we mutated conserved amino acid residues in the consensus sequence and compared the effects of these mutations in MTNR1A and MTNR1B.

We monitored MTNR1A signaling by utilizing the previously constructed yeast strain IMFD-70 (Togawa et al., 2010) containing two *EGFP* reporter genes and the re-engineered yeast strain IMFD-70ZsD (Nakamura et al., 2013a) containing two introduced *ZsGreen* reporter genes (Table 1). The expression of each of these reporter genes was controlled by the signal responsive *FIG1* promoter, allowing the detection of agonist-stimulated signal (Togawa et al., 2010). Human MTNR1A and MTNR1B receptors were previously reported to transduce signals in yeast cells through the

endogenous yeast Gα-subunit (Gpa1p) (Brown et al., 2000; Kokkola et al., 1998). We also used the yeast strain IMFD-72 (Ishii et al., 2012) and the re-engineered yeast strain IMFD-72ZsD (Nakamura et al., 2013a), which respectively contain two *EGFP* and *ZsGreen* reporter genes, as do the IMFD-70 and IMFD-72ZsD strains, but in which the carboxyl-terminal 5 amino acid residues of Gpa1p (KIGII) are replaced with the equivalent residues from human $G\alpha_{i3}$ (ECGLY) (Gpa1/$G\alpha_{i3}$ transplant, G_{i3}tp) (Table 1).

All four of these engineered yeast strains also harbor *ste2*Δ, *sst2*Δ and *far1*Δ alleles, thereby deleting the genes respectively encoding the yeast single GPCR (the yeast pheromone receptor: Ste2p), the yeast principal negative regulator of G-protein signaling (RGS: Sst2p), and the yeast G1-cyclin-dependent kinase inhibitor (which induces G1 cell cycle arrest in response to signal transduction (Far1p)) (Ishii et al., 2008 and 2012; Togawa et al., 2010). These deletions endow the strains with the following respective properties: allowing the cells to express human GPCRs in the absence of native yeast receptor, hypersensitizing agonist stimulation even at low

ligand concentrations, and continuing cell growth and plasmid retention despite receptor activation (due to the lack of G1 arrest).

It was previously reported that a yeast-human chimeric G-protein improved signal transduction via human MTNR1B in yeast (Brown et al., 2000). We tested the effects of replacing the fluorescent reporter gene and introducing the yeast-human chimeric G-protein in yeast cells expressing the human MTNR1A receptor by comparing the fluorescence of four types of yeast cells that express the combination of either *ZsGreen* or *EGFP* reporter gene and either yeast endogenous G-protein (Gpa1p) or the yeast-human chimeric G-protein (G_{i3}tp). The human MTNR1A and MTNR1B receptors were expressed via a multicopy episomal plasmid under the control of the constitutive *PGK1* promoter (pGK421-MTNR1A and pGK421-MTNR1B) (Table 1).

Yeast strains IMFD-70 (EGFP, Gpa1p), IMFD-72 (EGFP, G_{i3}tp), IMFD-70ZsD (ZsGreen, Gpa1p) and IMFD-72ZsD (ZsGreen, G_{i3}tp) harboring pGK421-MTNR1A (Table 1) were constructed and subjected to signaling assays. As shown in Figure 1A and Supporting Information Figure S1 and Figure S2, melatonin induced

dose-dependent increases in fluorescence intensities in all four strains. The half-maximal effective concentration (EC_{50}) values were 66 nM (IMFD-70), 20 nM (IMFD-72), 7.8 nM (IMFD-70ZsD) and 7.9 nM (IMFD-72ZsD). Although yeast strains IMFD-70 and IMFD-72 showed modest maximal percentage increases over the basal value (%E_{max}) (308%, IMFD-70; 367%, IMFD-72), the %E_{max} values of strains IMFD-70ZsD and IMFD-72ZsD were 6,531% and 9,159%, respectively (Figure 1A and Supporting Information Figure S1). These results indicated that the IMFD-72ZsD (ZsGreen, G_{i3}tp) strain expressing MTNR1A provided the highest fluorescence intensity and signal-to-noise (S/N) ratio, yielding a higher dynamic range and high sensitivity.

Using ZsGreen as a reporter clearly gave brighter green fluorescence and thus we constructed yeast strains IMFD-70ZsD (ZsGreen, Gpa1p) and IMFD-72ZsD (ZsGreen, G_{i3}tp) harboring pGK421-MTNR1B (Table 1) and subjected them to signaling assays. As shown in Figure 1B and Supporting Information Figure S2, melatonin-induced dose-dependent increases in fluorescence responses were confirmed in both MTNR1B-expressing strains, with EC_{50} values of 1.6 μM

(IMFD-70ZsD) and 1.1 μM (IMFD-72ZsD), giving %E_{max} values of 2,886% and 4,771%, respectively (Figure 1B). These results indicated that our IMFD-72ZsD-based system would be suitable for MTNR1A and MTNR1B signaling assays. Further studies were conducted using the yeast strain IMFD-72ZsD.

3.2. Examination of Relative Expression Levels and Localization of Mutated MTNR1A and MTNR1B

To test whether IMFD-72ZsD is appropriate for point mutation analysis of MTNR1A and MTNR1B, plasmids for the expression of 10 single and double mutants of MTNR1A and MTNR1B were constructed (Table 1). The 9 individual residues targeted within the MTNR1A and MTNR1B receptors are shown in Figure 2.

We compared the relative expression levels of the mutated MTNR1A- and MTNR1B-fused proteins by fusing a monomeric GFP (mUkG) reporter (Kaishima et al., 2016) to the C-termini of mutated MTNR1A and MTNR1B. The fluorescence intensities of cell suspensions of yeast expressing the mUkG-tagged MTNR1A- or MTNR1B-fused protein were measured (Figure 3). The fluorescence intensity measurements showed that all mUkG-tagged MTNR1A- and MTNR1B-fused

proteins were clearly expressed in yeast, and mutated MTNR1A and MTNR1B receptors were expressed at levels similar to that of wild-type MTNR1A and MTNR1B, respectively (Figure 3). In addition, the localization of several mutated MTNR1A- and MTNR1B-mUkG fusion proteins was observed using confocal laser scanning microscope (Figure 4). The mutated MTNR1A- and MTNR1B-mUkG fusion proteins localized to the cellular (plasma and endoplasmic reticulum) membranes similar to those of wild-type MTNR1A and MTNR1B, respectively (Figure 4).

3.3. Point Mutation Analysis of Human MTNR1A and MTNR1B Using the IMFD-72ZsD Yeast Strain

For point mutation analysis, we initially selected the D73N mutant of MTNR1A and the D86N mutant of MTNR1B. A conserved hydrophobic LAxxD motif located within the second transmembrane helix (TM2) of class A GPCRs is present in the TM2 of MTNR1A and MTNR1B, spanning from Leu69/82 to Asp73/86 (Ul-Haq et al., 2015). Conserved regions of the LAxxD motif are involved in ligand binding (Patny et al., 2006; Ul-Haq et al., 2015). As shown in Figures 5A and B, the abilities

of the D73N mutant of MTNR1A and the D86N mutant of MTNR1B expressed in yeast to promote melatonin-specific signaling were severely compromised. We previously reported that the D82N (LAxxD motif) mutation of serotonin HTR1A receptor abolished HTR1A signaling (Nakamura et al., 2015). Asp82 is spatially adjacent to Asn396 and is likely important for the proper function of HTR1A receptor (Sylte et al., 2001). Similarly, Asp73 (MTNR1A) and Asp86 (MTNR1B) are likely adjacent in space to Asn291 (MTNR1A) and Asp304 (MTNR1B) (Supporting Information Figure S3) and thus important for the proper function of melatonin receptors.

Many GPCRs form disulfide bridges between two cysteine residues in the third transmembrane helix (TM3) and the second extracellular loop (ECL2), and the resulting structure is important for ligand-dependent activation (Dohlman et al., 1990; Karnik et al., 2003; Klco et al., 2005). We previously suggested that the disulfide bond linking Cys113 and Cys190 is important for the structural conformation of the human MTNR1B receptor required to bind melatonin in HEK-293 cells (Mseeh et al., 2002). As expected, the MTNR1B C113A and C190A cysteine mutations effectively

abolished receptor signaling (Figure 5B). Our data obtained using yeast are overall consistent with the data shown in the 2002 report. Similarly, the MTNR1A C100A and C177A cysteine mutations were also severely compromised for signal activation in response to melatonin (Figure 5A).

Most members of the large family of rhodopsin-like GPCRs possess a highly conserved E/DRY motif in the C-terminal region of the third transmembrane domain (Rovati et al., 2007), whereas melatonin receptors have a conserved NRY sequence at the corresponding location (Kokkola et al., 2005). Several point mutation studies of MTNR1A have shown that Asn124 is important for MTNR1A melatonin receptor function (Kokkola et al., 1998 and 2003; Nelson et al., 2001). As shown in Figure 6A, the N124A and Y126A single mutations on MTNR1A showed drastically reduced agonist potencies and provided steep dose response curves (EC_{50} values of roughly 1.0 and 11 μM, respectively), although the maximal increases were similar to that of wild-type MTNR1A (%E_{max} of 10,831% and 8,708%, respectively). Thus, the results obtained with N124A were consistent with a previous report using yeast cells (Kokkola et al., 1998). In contrast, yeast strains expressing MTNR1A-R125A, and

MTNR1B-N137A, -R138A and -Y139A were severely compromised for signal activation in response to melatonin (Figures 6A and B).

The CWxP motif is strictly maintained in melatonin receptors, with a CWAP sequence spanning from Cys250/263 to Pro253/266 (MTNR1A/MTNR1B, respectively) (Pala et al., 2013). It was previously suggested that Pro253/266 are important for ligand binding and/or signaling of melatonin receptors in yeast and CHO-K1 cells, respectively (Kokkola et al., 1998; Mazna et al., 2008). Consistent with these reports, P253A (MTNR1A) and P266A (MTNR1B) substitutions impaired the functional response of the receptors, and the EC_{50} value of P253A (MTNR1A) was roughly 45 μM (Figures 7A and B). Taking the above mutational results together and comparing the consensus sequences of MTNR1A and MTNR1B, the mutations influenced receptor activities in similar manners.

Finally, we examined the effects of MTNR1A mutations (V192T, H195A, V192T+H195A) and MTNR1B mutations (V205T, H208A, V205T+H208A) for signaling activities using the IMFD-72ZsD yeast strain (Table 1). It was previously shown that MTNR1A-H195A exhibits increased agonist efficiencies in yeast cells

(Kokkola et al., 1998) whereas MTNR1B-H208A has reduced binding affinity for melatonin in HEK-293 cells (Gerdin et al., 2003). As shown in Figures 8A and B, MTNR1A-H195A exhibited increased agonist potency and MTNR1B-H208A retained partial activity, consistent with previous reports. The $\%E_{max}$ values for these mutants increased by 10,630% and 1,071%, and the EC_{50} values were roughly 0.00081 μM (0.81 nM) and 20 μM, respectively. Interestingly, even in the absence of melatonin, MTNR1A-H195A activated MTNR1A signaling (Figure 8A and Supporting Information Figure S4). This increase of basal (constitutive) signaling activity was not observed in yeast using *lacZ* (Kokkola et al., 1998) and suggests that our re-engineered yeast fluorescent GPCR biosensor has high sensitivity, enabling this increase in basal signaling activity to be detected. In addition, the yeast strains expressing MTNR1A-V192T and MTNR1B-V205T retained partial activities (Figures 8A and B). The $\%E_{max}$ values of these mutants increased by 9,228% and 3,406%, and the EC_{50} values were roughly 0.21 and 48 μM, respectively. Moreover, the double mutant V192T+H195A (MTNR1A) showed low constitutive activity whereas V205T+H208A (MTNR1B) was severely compromised for signal activation in response to melatonin (Figures 8A and B, and Supporting Information Figure S4).

The %E_{max} values for these mutants increased by 10,858% and 485%, and the EC_{50} values were roughly 0.0095 μM (9.5 nM) and 92 μM, respectively. Thus, comparison of the consensus sequences of MTNR1A (H195A) and MTNR1B (H208A) clearly showed different receptor activities arising from these mutations. As previous reported (Kokkola et al., 1998), the replacement of the basic and aromatic histidine residue with the smaller, aliphatic alanine residue at the position 195 of MTNR1A has changed the receptor conformation to increase the agonist potency and basal activity. In contrast, the replacement of the histidine residue at the position 208 of MTNR1B might have negatively affected the change in the receptor conformation, thus probably descreasing the binding of melatonin. These results strongly suggested that the IMFD-72ZsD yeast strain is useful for the screening and identification of amino acid residues critical for the signaling activity of melatonin receptors. In addition, because *S. cerevisiae* can functionally express a variety of human GPCRs (Ishii et al., 2010; Minic et al., 2005), our yeast fluorescent biosensor can be readily adapted for assaying other human GPCRs.

4. Conclusion

In this study, we constructed a fluorescence-based yeast biosensor that can monitor the activation of human melatonin receptor signaling in response to melatonin. This biosensor incorporates a fluorescent reporter (*ZsGreen*) and a chimeric yeast-human Gα protein, yielding higher dynamic range and high sensitivity compared to other biosensors. We adapted this yeast biosensor for comparative point mutation analysis between human MTNR1A and MTNR1B melatonin receptors (Table 2). Most mutations in the consensus sequences significantly affected the signaling capacities of both receptors, although there were differences between these subtype receptors (Table 2). Further analysis of the functions of mutations in melatonin receptors could help elucidate the mechanism of the disorders such as type-2 diabetes and Parkinson's disease. This biosensor may help reveal the functions of melatonin receptors and aid in the development of novel and more efficacious therapeutic agents.

Acknowledgements

This work was supported by JSPS KAKENHI Grant Numbers JP17K17878 and JP19K15734. Funding was also provided by Project Focused on Developing Key

Technology for Discovering and Manufacturing Drugs for Next-Generation Treatment and Diagnosis from the Agency for Medical Research and Development (AMED) of Japan [Grant Numbers JP19ae0101055 and JP19ae0101060].

Conflicts of Interest

The authors declare no commercial or financial conflicts of interest.

Author Contributions

Yasuyuki Nakamura, and Jun Ishii conceived and designed the experiments. Yasuyuki Nakamura, Ririka Asama, and Takuya Tabata performed experiments. Yasuyuki Nakamura and Jun Ishii analyzed data. Kenta Morita and Tatsuo Maruyama participated in experiment of confocal imaging. Akihiko Kondo and Jun Ishii supervised the research. Yasuyuki Nakamura and Jun Ishii wrote the manuscript. All authors read and approved the manuscript.

References

Abreu T, Bragança M. 2015. The bipolarity of light and dark: A review on Bipolar Disorder and circadian cycles. *Journal of Affective Disorders* 185:219–229.

Adi N, Mash DC, Ali Y, Singer C, Shehadeh L, Papapetropoulos S. 2010. Melatonin MT1 and MT2 receptor expression in Parkinson's disease. *Med Sci Monit* **16**:BR61–67.

Blask DE, Sauer LA, Dauchy RT, Holowachuk EW, Ruhoff MS, Kopff HS. 1999. Melatonin inhibition of cancer growth in vivo involves suppression of tumor fatty acid metabolism via melatonin receptor-mediated signal transduction events. *Cancer Res*. **59**:4693–4701.

Bonnefond A, Clément N, Fawcett K, Yengo L, Vaillant E, Guillaume JL, Dechaume A, Payne F, Roussel R, Czernichow S, Hercberg S, Hadjadj S, Balkau B, Marre M, Lantieri O, Langenberg C, Bouatia-Naji N, Charpentier G, Vaxillaire M, Rocheleau G, Wareham NJ, Sladek R, McCarthy MI, Dina C, Barroso I, Jockers R, Froguel P. 2012. Rare MTNR1B variants impairing melatonin receptor 1B function contribute to type 2 diabetes. *Nature Genetics* **44**:297–301.

Brachmann CB, Davies A, Cost GJ, Caputo E, Li J, Hieter P, Boeke JD. 1998. Designer deletion strains derived from *Saccharomyces cerevisiae* S288C: a useful set of strains and plasmids for PCR-mediated gene disruption and other applications. Yeast 14(2):115–132.

Brown AJ, Dyos SL, Whiteway MS, White JHM, Watson MAEA, Marzioch M, Clare JJ, Cousens DJ, Paddon C, Plumpton C, Romanos MA, Dowell SJ. 2000. Functional coupling of mammalian receptors to the yeast mating pathway using novel yeast/mammalian G protein α-subunit chimeras. *Yeast* **16**:11–22.

Delagrange P, Atkinson ÃJ, Boutin JA, Casteilla ÃL, Lesieur D, Misslin R, Pellissier S, Pé ÃL, Renard P. 2003. Therapeutic Perspectives for Melatonin Agonists and Antagonists. *J Neuroendocrinol* **15**:442–448.

Dohlman HG, Caron MG, DeBlasi A, Frielle T, Lefkowitz RJ. 1990. Role of extracellular disulfide-bonded cysteines in the ligand binding function of the beta 2-adrenergic receptor. *Biochemistry*. **29**:2335–2342.

Dubocovich ML, Delagrange P, Krause DN, Sugden D, Cardinali DP, Olcese J. 2010. International union of basic and clinical pharmacology. LXXV. Nomenclature,

classification, and pharmacology of G protein-coupled melatonin receptors. *Pharmacological Reviews*. 62:343–380.

Ge W bo, Xiao L fei, Duan H wei, Li Z shuai, Jiang Y ting, Yang S shan, Hu J jie, Zhang Y, Zhao X xu. 2019. Melatonin protects against lipopolysaccharide-induced epididymitis in sheep epididymal epithelial cells in vitro. *Immunology Letters* **214**:45–51.

Gerdin MJ, Mseeh F, Dubocovich ML. 2003. Mutagenesis studies of the human MT2 melatonin receptor. *Biochemical Pharmacology* **66**:315–320.

Gietz D, St Jean A, Woods RA, Schiestl RH. 1992. Improved method for high efficiency transformation of intact yeast cells. *Nucl Acid Res* **20**:1425.

Gobbi G, Comai S. 2019. Differential function of melatonin MT1 and MT2 receptors in REM and NREM sleep. *Front Endocrinol (Lausanne)* **10**:87.

Hashi H, Nakamura Y, Ishii J, Kondo A. 2018. Modifying Expression Modes of Human Neurotensin Receptor Type 1 Alters Sensing Capabilities for Agonists in Yeast Signaling Biosensor. *Biotechnology Journal* **13**:e1700522.

Ishii J, Matsumura S, Kimura S, Tatematsu K, Kuroda S, Fukuda H, Kondo A. 2006. Quantitative and dynamic analyses of G protein-coupled receptor signaling in yeast using Fus1, enhanced green fluorescence protein (EGFP), and His3 fusion protein. *Biotechnology Progress* **22**:954–960.

Ishii J, Tanaka T, Matsumura S, Tatematsu K, Kuroda S, Ogino C, Fukuda H, Kondo A. 2008. Yeast-based fluorescence reporter assay of G protein-coupled receptor signalling for flow cytometric screening: FAR1-disruption recovers loss of episomal plasmid caused by signalling in yeast. *Journal of Biochemistry* **143**:667–674.

Ishii J, Fukuda N, Tanaka T, Ogino C, Kondo A. 2010. Protein-protein interactions and selection: Yeast-based approaches that exploit guanine nucleotide-binding protein signaling. *FEBS Journal*. **277**:1982–1995.

Ishii J, Moriguchi M, Hara KY, Shibasaki S, Fukuda H, Kondo A. 2012. Improved identification of agonist-mediated Gαi-specific human G-protein-coupled receptor signaling in yeast cells by flow cytometry. *Analytical Biochemistry* **426**:129–133.

Ishii J, Oda A, Togawa S, Fukao A, Fujiwara T, Ogino C, Kondo A. 2014. Microbial fluorescence sensing for human neurotensin receptor type 1 using Gα-engineered yeast cells. *Analytical Biochemistry* **446**:37–43.

Johansson LC, Stauch B, McCorvy JD, Han GW, Patel N, Huang XP, Batyuk A, Gati C, Slocum ST, Li C, Grandner JM, Hao S, Olsen RHJ, Tribo AR, Zaare S, Zhu L, Zatsepin NA, Weierstall U, Yous S, Stevens RC, Liu W, Roth BL, Katritch V, Cherezov V. 2019. XFEL structures of the human MT2 melatonin receptor reveal the basis of subtype selectivity. *Nature* **569**:289–292.

Kaishima M, Ishii J, Matsuno T, Fukuda N, Kondo A. 2016. Expression of varied GFPs in Saccharomyces cerevisiae: codon optimization yields stronger than expected expression and fluorescence intensity. *Scientific Reports* **6**:35932.

Karnik SS, Gogonea C, Patil S, Saad Y, Takezako T. 2003. Activation of G-protein-coupled receptors: a common molecular mechanism. *Trends in Endocrinology & Metabolism* **14**:431–437.

Kinoshita K, Nakamura H. 2004. eF-site and PDBjViewer: Database and viewer for protein functional sites. *Bioinformatics* **20**:1329–1330.

Klco JM, Wiegand CB, Narzinski K, Baranski TJ. 2005. Essential role for the second extracellular loop in C5a receptor activation. *Nature Structural and Molecular Biology* **12**:320–326.

Klco JM, Nikiforovich G v., Baranski TJ. 2006. Genetic analysis of the first and third extracellular loops of the C5a receptor reveals an essential WXFG motif in the first loop. *Journal of Biological Chemistry* **281**:12010–12019.

Kokkola T, Watson M-A, White J, Dowell S, Foord SM, Laitinen JT. 1998. Mutagenesis of Human Mel 1a Melatonin Receptor Expressed in Yeast Reveals

Domains Important for Receptor Function. *Biochemical and Biophysical Research Communications*. **249**:531–536.

Kokkola T, Foord SM, Watson MA, Vakkuri O, Laitinen JT. 2003. Important amino acids for the function of the human MT1 melatonin receptor. *Biochemical Pharmacology* **65**:1463–1471.

Kokkola T, Salo OMH, Poso A, Laitinen JT. 2005. The functional role of cysteines adjacent to the NRY motif of the human MT1 melatonin receptor. *Journal of Pineal Research* **39**:1–11.

Liu R, Wong W, IJzerman AP. 2016. Human G protein-coupled receptor studies in Saccharomyces cerevisiae. *Biochemical Pharmacology* **114**:103–115.

Lyssenko V, Nagorny CLF, Erdos MR, Wierup N, Jonsson A, Spégel P, Bugliani M, Saxena R, Fex M, Pulizzi N, Isomaa B, Tuomi T, Nilsson P, Kuusisto J, Tuomilehto J, Boehnke M, Altshuler D, Sundler F, Eriksson JG, Jackson AU, Laakso M, Marchetti P, Watanabe RM, Mulder H, Groop L. 2009. Common variant in MTNR1B associated with increased risk of type 2 diabetes and impaired early insulin secretion. *Nature Genetics* **41**:82–88.

Martínez-Campa C, González A, Mediavilla MD, Alonso-González C, Alvarez-García V, Sánchez-Barcelo EJ, Cos S. 2009. Melatonin inhibits aromatase promoter expression by regulating cyclooxygenases expression and activity in breast cancer cells. *Br J Cancer*. **101**:1613-1619.

Mazna P, Grycova L, Balik A, Zemkova H, Friedlova E, Obsilova V, Obsil T, Teisinger J. 2008. The role of proline residues in the structure and function of human MT2 melatonin receptor. *Journal of Pineal Research* **45**:361–372.

Miller E, Morel A, Saso L, Saluk J. 2015. Melatonin redox activity. Its potential clinical applications in neurodegenerative disorders. *Curr Top Med Chem*. **15**:163-169.

Minic J, Sautel M, Salesse R, Pajot-Augy E. 2005. Yeast system as a screening tool for pharmacological assessment of g protein coupled receptors. *Current medicinal chemistry* **12**:961–969.

Mseeh F, Gerdin MJ, Dubocovich ML. 2002. Identification of cysteines involved in ligand binding to the human melatonin MT2 receptor. *European Journal of Pharmacology* **449**:29–38.

Nakamura Y, Ishii J, Kondo A. 2013a. Bright fluorescence monitoring system utilizing zoanthus sp. green fluorescent protein (ZsGreen) for human g-protein-coupled receptor signaling in microbial yeast cells. *PLoS ONE* **8**:e82237.

Nakamura Y, Ishii J, Kondo A. 2013b. Rapid, Facile Detection of Heterodimer Partners for Target Human G-Protein-Coupled Receptors Using a Modified Split-Ubiquitin Membrane Yeast Two-Hybrid System. *PLoS ONE* **8**:e66793.

Nakamura Y, Ishii J, Kondo A. 2014. Construction of a yeast-based signaling biosensor for human angiotensin II type 1 receptor via functional coupling between Asn295-mutated receptor and Gpa1/Gi3 chimeric G?? *Biotechnology and Bioengineering* **111**:2220–2228.

Nakamura Y, Ishii J, Kondo A. 2015. Applications of yeast-based signaling sensor for characterization of antagonist and analysis of site-directed mutants of the human serotonin 1A receptor. *Biotechnology and Bioengineering* **112**:1906–1915.

Nelson CS, Ikeda M, Gompf HS, Robinson ML, Fuchs NK, Yoshioka T, Neve KA, Allen CN. 2001. Regulation of Melatonin 1a Receptor Signaling and Trafficking by Asparagine-124. *Molecular Endocrinology* **15**:1306–1317.

Pala D, Lodola A, Bedini A, Spadoni G, Rivara S. 2013. Homology models of melatonin receptors: Challenges and recent advances. *International Journal of Molecular Sciences*. **14**:8093–8121.

Pandi-Perumal SR, Srinivasan V, Maestroni GJ, Cardinali DP, Poeggeler B, Hardeland R. 2006. Melatonin: Nature's most versatile biological signal?. *FEBS J*. **273**:2813-2838.

Pandi-Perumal SR, Trakht I, Srinivasan V, Spence DW, Maestroni GJM, Zisapel N, Cardinali DP. 2008. Physiological effects of melatonin: role of melatonin receptors and signal transduction pathways. *Prog Neurobiol*. **85**:335-353.

Patny A, Desai PV, Avery MA. 2006. Homology modeling of G-protein-coupled receptors and implications in drug design. *Curr Med Chem*. **13**:1667-1691.

Reiter RJ. 1991. Pineal Melatonin: Cell Biology of Its Synthesis and of Its Physiological Interactions. *Endocrine Reviews* **12**:151–180.

Reppert SM, Weaver DR, Ebisawa T. 1994. Cloning and Characterization of a Mammalian Melatonin Receptor That Mediates Reproductive and Circadian Responses. *Neuron*. **13**:1177–1185.

Reppert SM, Godson C, Mahlet CD, Weaver DR, Slaugenhaupt SA, Gusella JF. 1995. Molecular characterization of a second melatonin receptor expressed in human retina and brain: The Mellb melatonin receptor. *Proc. Nati. Acad. Sci. USA*. **92**:8734–8738.

Rosenbaum DM, Cherezov V, Hanson MA, Rasmussen SGF, Thian FS, Kobilka TS, Choi HJ, Yao XJ, Weis WI, Stevens RC, Kobilka BK. 2007. GPCR Engineering Yields High-Resolution Structural Insights Into beta2-adrenergic Receptor Function. *Science* **318**:1266–1273.

Rovati GE, Capra V, Neubig RR. 2007. The highly conserved DRY motif of class A G protein-coupled receptors: beyond the ground state. *Mol Pharmacol*. **71**:959-964.

Scarselli M, Li B, Kim SK, Wess J. 2007. Multiple residues in the second extracellular loop are critical for M3 muscarinic acetylcholine receptor activation. *Journal of Biological Chemistry* **282**:7385–7396.

Simonneaux V, Ribelayga C. 2003. Generation of the melatonin endocrine message in mammals: a review of the complex regulation of melatonin synthesis by norepinephrine, peptides, and other pineal transmitters. *Pharmacol Rev*. **55**:325-395.

Stauch B, Johansson LC, McCorvy JD, Patel N, Han GW, Huang XP, Gati C, Batyuk A, Slocum ST, Ishchenko A, Brehm W, White TA, Michaelian N, Madsen C, Zhu L, Grant TD, Grandner JM, Shiriaeva A, Olsen RHJ, Tribo AR, Yous S, Stevens RC, Weierstall U, Katritch V, Roth BL, Liu W, Cherezov V. 2019.

Structural basis of ligand recognition at the human MT1 melatonin receptor. *Nature* **569**:284–288.

Sylte I, Bronowska A, Dahl SG. 2001. Ligand induced conformational states of the 5-HT1A receptor. *European Journal of Pharmacology* **416**:33–41.

Togawa S, Ishii J, Ishikura A, Tanaka T, Ogino C, Kondo A. 2010. Importance of asparagine residues at positions 13 and 26 on the amino-terminal domain of human somatostatin receptor subtype-5 in signalling. *Journal of Biochemistry* **147**:867–873.

Ul-Haq Z, Saeed M, Halim SA, Khan W. 2015. 3D structure prediction of human β1-adrenergic receptor via threading-based homology modeling for implications in structure-based drug designing. *PLoS ONE* **10**:e0122223.

Vriend J, Reiter RJ. 2015. Breast cancer cells: Modulation by melatonin and the ubiquitin-proteasome system - A review. *Molecular and Cellular Endocrinology*. **417**:1–9.

Zawilska JB, Skene DJ, Arendt J. 2009. Physiology and pharmacology of melatonin in relation to biological rhythms. *Pharmacol Rev* **61**:383–410.

Zlotos DP, Jockers R, Cecon E, Rivara S, Witt-Enderby PA. 2014. MT1 and MT2 melatonin receptors: Ligands, models, oligomers, and therapeutic potential. *Journal of Medicinal Chemistry* **57**:3161–3185.

Table 1. **Yeast strains and plasmids used in this study.**

Strain or plasmid	Specific features	Source
Strain		
BY4741	*MAT***a** *his3Δ1 leu2Δ0 met15Δ0 ura3Δ0*	Brachmann et al. (1998)

IMFD-70	BY4741 *sst2*Δ::*AUR1-C ste2*Δ::*LEU2 fig1*Δ::*EGFP his3*Δ::P_{FIG1}-*EGFP far1*Δ	Togawa et al. (2010)
IMFD-72	BY4741 *sst2*Δ::*AUR1-C ste2*Δ::*LEU2 fig1*Δ::*EGFP his3*Δ::P_{FIG1}-*EGFP far1*Δ *gpa1*Δ::G_{i3}*tp*	Ishii et al. (2012)
IMFD-70ZsD	BY4741 *sst2*Δ::*AUR1-C ste2*Δ::*LEU2 fig1*Δ::*ZsGreen his3*Δ::P_{FIG1}-*ZsGreen far1*Δ	Nakamura et al. (2013a)
IMFD-72ZsD	BY4741 *sst2*Δ::*AUR1-C ste2*Δ::*LEU2 fig1*Δ::*ZsGreen his3*Δ::P_{FIG1}-*ZsGreen far1*Δ *gpa1*Δ::G_{i3}*tp*	Nakamura et al. (2013a)
Plasmid		
pGK421	Yeast expression vector containing *PGK1* promoter, *PGK1* terminator, 2μ origin and *MET15* marker	Togawa et al. (2010)
pGK421-MTNR1A	Human MTNR1A receptor expression in pGK421	This study
pGK421-MTNR1B	Human MTNR1B receptor expression in pGK421	This study
pGK421-MTNR1A-D73N	Human MTNR1A receptor (D73N) mutant expression in pGK421	This study
pGK421-MTNR1A-C100A	Human MTNR1A receptor (C100A) mutant	This study

	expression in pGK421	
pGK421-MTNR1A-N124A	Human MTNR1A receptor (N124A) mutant expression in pGK421	This study
pGK421-MTNR1A-R125A	Human MTNR1A receptor (R125A) mutant expression in pGK421	This study
pGK421-MTNR1A-Y126A	Human MTNR1A receptor (Y126A) mutant expression in pGK421	This study
pGK421-MTNR1A-C177A	Human MTNR1A receptor (C177A) mutant expression in pGK421	This study
pGK421-MTNR1A-V192T	Human MTNR1A receptor (V192T) mutant expression in pGK421	This study
pGK421-MTNR1A-H195A	Human MTNR1A receptor (H195A) mutant expression in pGK421	This study
pGK421-MTNR1A-V192T-H195A	Human MTNR1A receptor (V192T-H195A) mutant expression in pGK421	This study
pGK421-MTNR1A-P253A	Human MTNR1A receptor (P253A) mutant expression in pGK421	This study
pGK421-MTNR1B-D86N	Human MTNR1B receptor (D86N) mutant expression in pGK421	This study
pGK421-MTNR1B-C113A	Human MTNR1B receptor (C113A) mutant expression in pGK421	This study
pGK421-MTNR1B-N137A	Human MTNR1B receptor	This study

	(N137A) mutant expression in pGK421	
pGK421-MTNR1B-R138A	Human MTNR1B receptor (R138A) mutant expression in pGK421	This study
pGK421-MTNR1B-Y139A	Human MTNR1B receptor (Y139A) mutant expression in pGK421	This study
pGK421-MTNR1B-C190A	Human MTNR1B receptor (C190A) mutant expression in pGK421	This study
pGK421-MTNR1B-V205T	Human MTNR1B receptor (V205T) mutant expression in pGK421	This study
pGK421-MTNR1B-H208A	Human MTNR1B receptor (H208A) mutant expression in pGK421	This study
pGK421-MTNR1B-V205T-H208A	Human MTNR1B receptor (V205T-H208A) mutant expression in pGK421	This study
pGK421-MTNR1B-P266A	Human MTNR1B receptor (P266A) mutant expression in pGK421	This study
pGK421-MTNR1A-mUkG	mUkG-fused human MTNR1A receptor expression in pGK421	This study
pGK421-MTNR1B-mUkG	mUkG-fused human MTNR1B receptor expression in pGK421	This study
pGK421-MTNR1A-D73N-mUkG	mUkG-fused human MTNR1A receptor (D73N) mutant expression in pGK421	This study

pGK421-MTNR1A-C100A-mUkG	mUkG-fused human MTNR1A receptor (C100A) mutant expression in pGK421	This study
pGK421-MTNR1A-N124A-mUkG	mUkG-fused human MTNR1A receptor (N124A) mutant expression in pGK421	This study
pGK421-MTNR1A-R125A-mUkG	mUkG-fused human MTNR1A receptor (R125A) mutant expression in pGK421	This study
pGK421-MTNR1A-Y126A-mUkG	mUkG-fused human MTNR1A receptor (Y126A) mutant expression in pGK421	This study
pGK421-MTNR1A-C177A-mUkG	mUkG-fused human MTNR1A receptor (C177A) mutant expression in pGK421	This study
pGK421-MTNR1A-V192T-mUkG	mUkG-fused human MTNR1A receptor (V192T) mutant expression in pGK421	This study
pGK421-MTNR1A-H195A-mUkG	mUkG-fused human MTNR1A receptor (H195A) mutant expression in pGK421	This study
pGK421-MTNR1A-V192T-H195A-mUkG	mUkG-fused human MTNR1A receptor (V192T-H195A) mutant expression in pGK421	This study
pGK421-MTNR1A-P253A-mUkG	mUkG-fused human	This study

	MTNR1A receptor (P253A) mutant expression in pGK421	
pGK421-MTNR1B-D86N-mUkG	mUkG-fused human MTNR1B receptor (D86N) mutant expression in pGK421	This study
pGK421-MTNR1B-C113A-mUkG	mUkG-fused human MTNR1B receptor (C113A) mutant expression in pGK421	This study
pGK421-MTNR1B-N137A-mUkG	mUkG-fused human MTNR1B receptor (N137A) mutant expression in pGK421	This study
pGK421-MTNR1B-R138A-mUkG	mUkG-fused human MTNR1B receptor (R138A) mutant expression in pGK421	This study
pGK421-MTNR1B-Y139A-mUkG	mUkG-fused human MTNR1B receptor (Y139A) mutant expression in pGK421	This study
pGK421-MTNR1B-C190A-mUkG	mUkG-fused human MTNR1B receptor (C190A) mutant expression in pGK421	This study
pGK421-MTNR1B-V205T-mUkG	mUkG-fused human MTNR1B receptor (V205T) mutant expression in pGK421	This study
pGK421-MTNR1B-H208A-mUkG	mUkG-fused human MTNR1B receptor	This study

	(H208A) mutant expression in pGK421	
pGK421-MTNR1B-V205T-H208A-mUkG	mUkG-fused human MTNR1B receptor (V205T-H208A) mutant expression in pGK421	This study
pGK421-MTNR1B-P266A-mUkG	mUkG-fused human MTNR1B receptor (P266A) mutant expression in pGK421	This study

Table 2. **Summary of comparative point mutation analysis between MTNR1A and MTNR1B using the IMFD-72ZsD yeast strain.**

EC_{50} [nM]				**%E_{max}**			
MTNR1A		**MTNR1B**		**MTNR1A**		**MTNR1B**	
WT	7.9	WT	1.1×10^3	WT	9159 ± 169	WT	4771 ± 121
D73N	3.0×10^4	D86N	n.d.	D73N	83 ± 42	D86N	n.d.
C100A	n.d.	C113A	n.d.	C100A	7745 ± 38*	C113A	n.d.

C177A	n.d.	C190A	n.d.	C177A	6291 ± 401*	C190A	n.d.
N124A	1.0×10^3	N137A	n.d.	N124A	10831 ± 219	N137A	1366 ± 34*
R125A	n.d.	R138A	n.d.	R125A	1174 ± 121*	R138A	n.d.
Y126A	1.1×10^4	Y139A	n.d.	Y126A	8708 ± 309	Y139A	1171 ± 41*
P253A	n.d.	P266A	n.d.	P253A	9589 ± 238*	P266A	2185 ± 34*
V192T	2.1×10^2	V205T	n.d.	V192T	9228 ± 207	V205T	3406 ± 95*
H195A	0.81	H208A	2.0×10^4	H195A	10630 ± 506	H208A	1071 ± 53
V192T + H195A	9.5	V205T + H208A	9.2×10^4	V192T + H195A	10858 ± 553	V205T + H208A	485 ± 14

n.d. = not determined

* These %E_{max} values have not reached saturation.

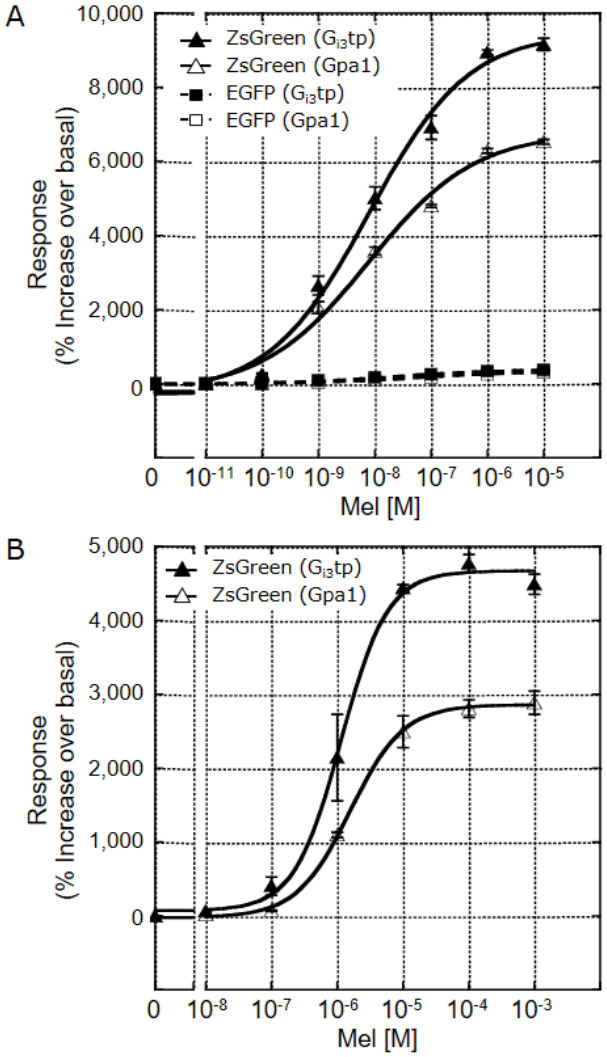

Figure 1. MTNR1A and MTNR1B-based melatonin biosensor dose-response curves in recombinant yeast cells. (A) Yeast strains IMFD-70 (EGFP (Gpa1)), IMFD-72 (EGFP (G_{i3}tp)), IMFD-70ZsD (ZsGreen (Gpa1)) and IMFD-72ZsD (ZsGreen (G_{i3}tp)) transformed with pGK421-MTNR1A. (B) Yeast strains IMFD-70ZsD (ZsGreen (Gpa1)) and IMFD-72ZsD (ZsGreen (G_{i3}tp)) transformed with pGK421-MTNR1B. All transformants were grown in SD selective medium for 18 h. The cells were then incubated for another 4 h in pH-adjusted SD selective medium supplemented with melatonin (Mel) at various concentrations. The mean GFP fluorescence of 10,000 cells was measured by flow cytometry. Each data point represents the mean ± standard deviation of three independent transformants (n = 3).

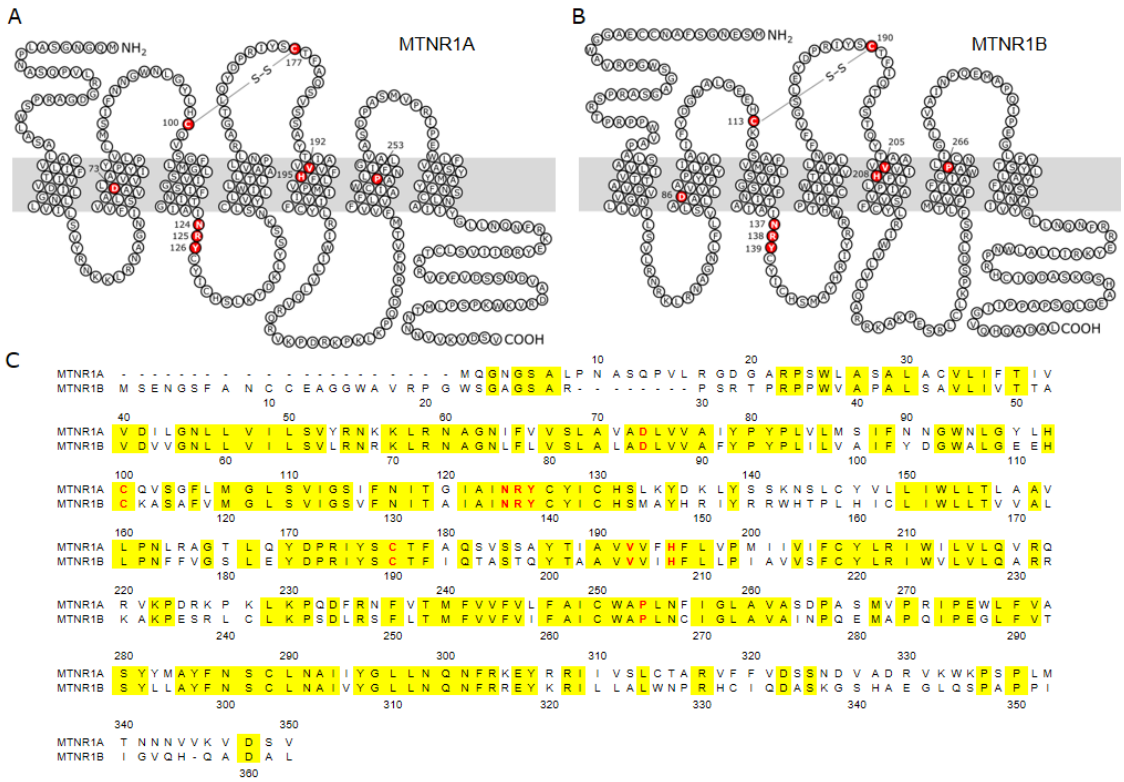

Figure 2. Schematic illustration of human (A) MTNR1A and (B) MTNR1B receptors, showing the positions of the analyzed mutations. Each circle represents an amino acid residue. The positions of the amino acids mutated in this study are indicated as red circles. (C) Comparison of the amino acid sequences of human MTNR1A and MTNR1B receptors. The red amino acids indicate the residues mutated in this study. Yellow background indicates identical amino acids in the two sequences.

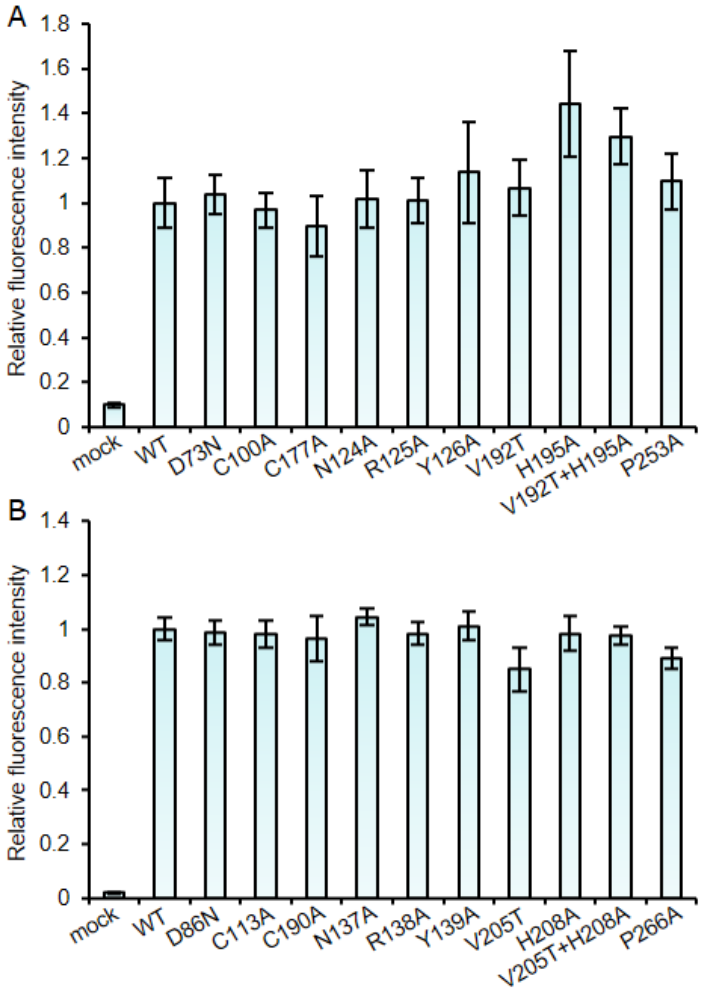

Figure 3. The relative expression levels of wild-type (WT) and mutant MTNR1A and MTNR1B receptors fused with a green fluorescent protein (mUkG) at the carboxyl-termini. Yeast strain IMFD-72ZsD was transformed with pGK421 (mock), pGK421-MTNR1A-mUkG-based plasmids (WT MTNR1A or its mutants) (A) or pGK421-MTNR1B-mUkG-based plasmids (WT MTNR1B or its mutants) (B). All transformants were grown in SD selective media for 18 h. The mean mUkG fluorescence of 10,000 cells was measured by flow cytometry. Error bars represent the standard deviation from three independent transformants (n = 3).

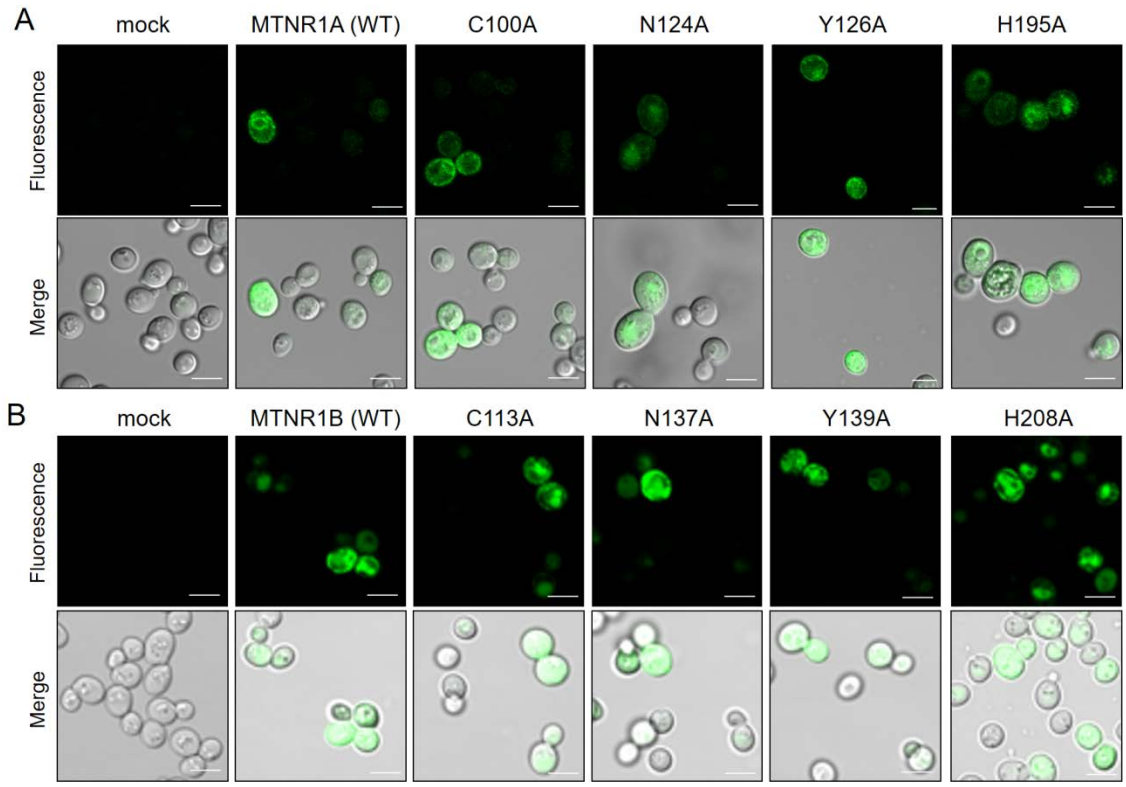

Figure 4. Confocal images of yeast strain BY4741 harboring pGK421 (mock), pGK421-MTNR1A-mUkG-based plasmids (WT MTNR1A or its mutants) (A) or pGK421-MTNR1B-mUkG-based plasmids (WT MTNR1B or its mutants) (B). A confocal laser scanning microscope (CLSM; FV3000-IX83, Olympus) was used for obtaining green fluorescence and differential interference images. All transformants were grown in SD selective media for 18 h. The upper photographs are fluorescence micrographs, and the lower photographs are merged fluorescence and differential interference micrographs. Scale bar: 5 μm.

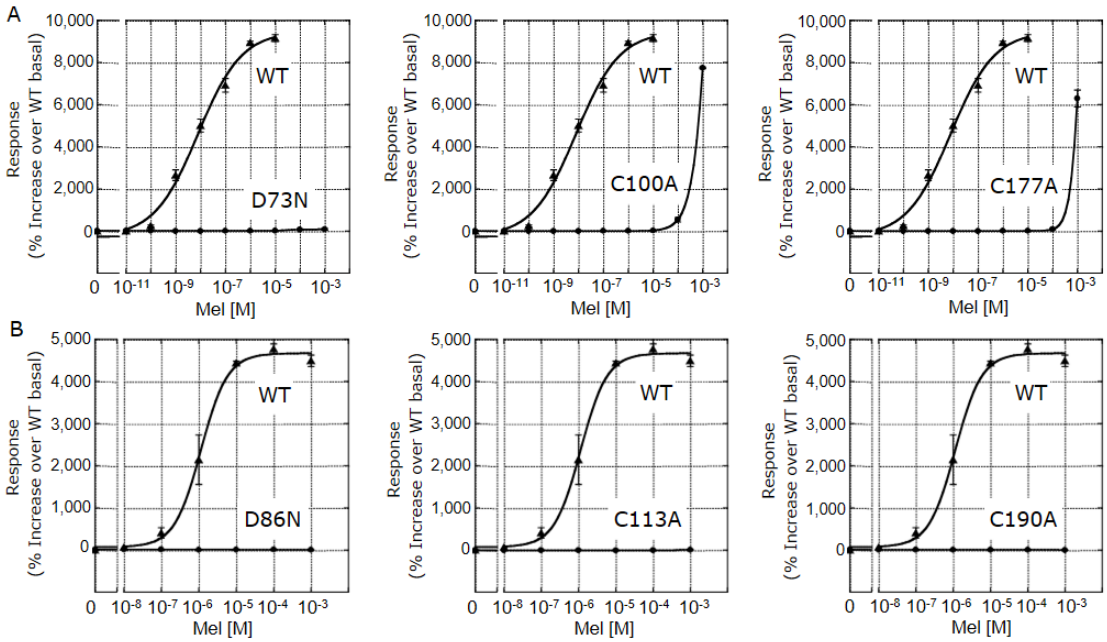

Figure 5. Ligand response of wild-type (WT) and mutant (A) MTNR1A (D73N, C100A, C177A) and (B) MTNR1B (D86N, C113A, C190A) receptors. The dose-response relationship to melatonin (Mel) was determined using recombinant yeast strain IMFD-72ZsD (ZsGreen (G_{i3}tp)) expressing WT or mutant receptor. All transformants were grown in SD selective medium for 18 h. The cells were then incubated for another 4 h in pH-adjusted SD selective medium supplemented with Mel at various concentrations. The mean ZsGreen fluorescence of 10,000 cells was measured by flow cytometry. Each data point represents the mean ± standard deviation of three independent transformants (n = 3).

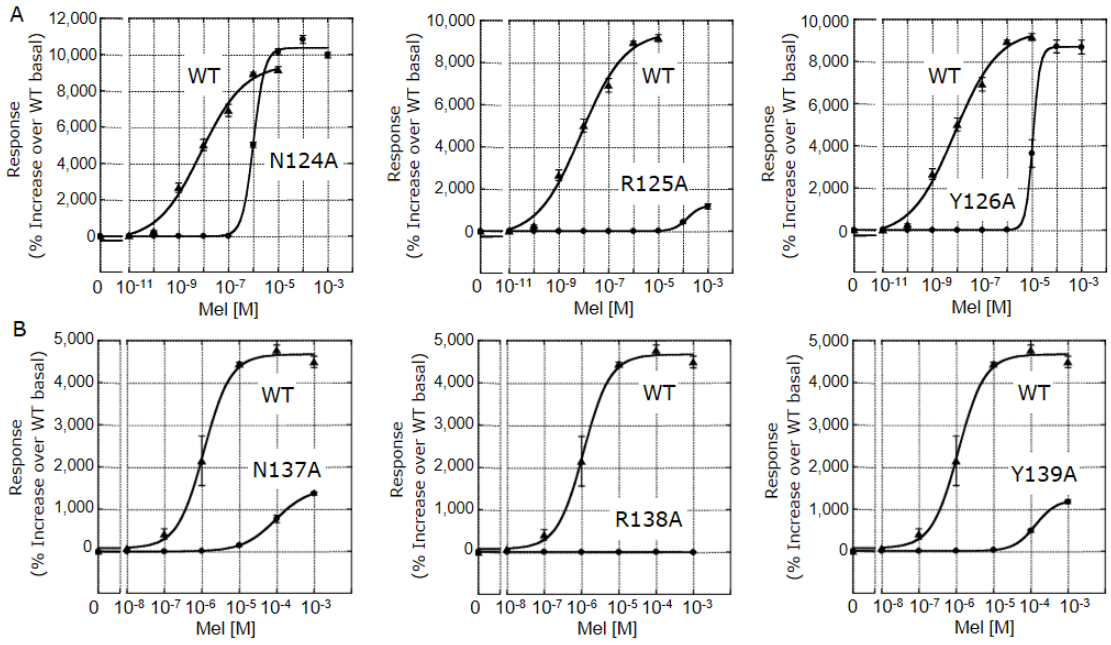

Figure 6. Ligand response of wild-type (WT) and mutant (A) MTNR1A (N124A, R125A, Y126A) and (B) MTNR1B (N137A, R138A, Y139A) receptors. The dose-response relationship to melatonin (Mel) was determined using recombinant yeast strain IMFD-72ZsD (ZsGreen (G_{i3}tp)) expressing WT or mutant receptor. The transformants were grown in SD selective medium for 18 h. The cells were then incubated for another 4 h in pH-adjusted SD selective medium supplemented with Mel at various concentrations. The mean ZsGreen fluorescence of 10,000 cells was measured by flow cytometry. Each data point represents the mean ± standard deviation of three independent transformants (n = 3).

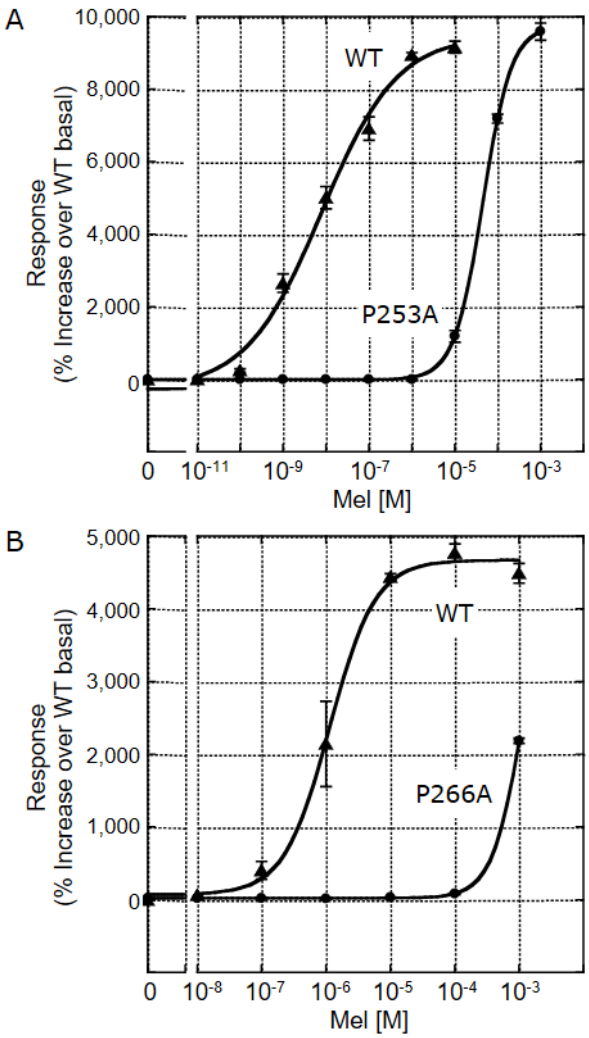

Figure 7. Ligand response of wild-type (WT) and mutant (A) MTNR1A (P253A) and (B) MTNR1B (P266A) receptors. The dose-response relationship to melatonin (Mel) was determined using recombinant yeast strain IMFD-72ZsD (ZsGreen (G_{i3}tp)) expressing WT or mutant receptor. The transformants were grown in SD selective medium for 18 h. The cells were then incubated for another 4 h in pH-adjusted SD selective medium supplemented with Mel at various concentrations. The mean ZsGreen fluorescence of 10,000 cells was measured by flow cytometry. Each data point represents the mean ± standard deviation of three independent transformants (*n* = 3).

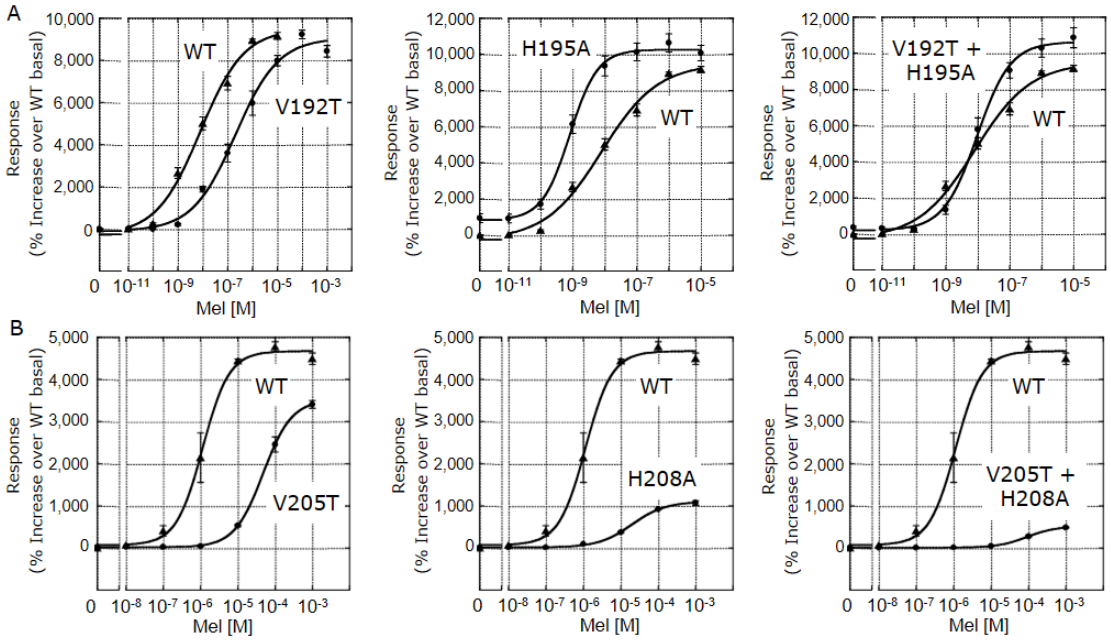

Figure 8. Ligand response of wild-type (WT) and mutant (A) MTNR1A (V192T, H195A, V192T+H195A) and (B) MTNR1B (V205T, H208A, V205T+H208A) receptors. The dose-response relationship to melatonin was determined using recombinant yeast strain IMFD-72ZsD (ZsGreen (G_{i3}tp)) expressing WT or mutant receptor. The transformants were grown in SD selective medium for 18 h. The cells were then incubated for another 4 h in pH-adjusted SD selective medium supplemented with melatonin at various concentrations. The mean ZsGreen fluorescence of 10,000 cells was measured by flow cytometry. The data shown represent the mean ± standard deviation of three independent transformants (n = 3).